Engineering with Computers (2022) 38 (Suppl 3):S2205–S2228
https://doi.org/10.1007/s00366-021-01378-8

ORIGINAL ARTICLE

Inverse problem for dynamic structural health monitoring based on slime mould algorithm

Samir Tiachacht[1] · Samir Khatir[2,3] · Cuong Le Thanh[3] · Ravipudi Venkata Rao[4] · Seyedali Mirjalili[5,6] · Magd Abdel Wahab[7,8]

Received: 25 November 2020 / Accepted: 27 February 2021 / Published online: 22 March 2021

Abstract
In this paper, damage detection, localization and quantification are performed using modal strain energy change ratio (MSEcr) as damage indicator combined with a new optimization technique, namely slime mould algorithm (SMA) developed in 2020. The SMA algorithm is employed to assess structural damage and monitor structural health. Two structures, including a laboratory beam and a bar planar truss are considered to study the effectiveness of the proposed approach. Another recent algorithm called marine predators algorithm (MPA) is also used for comparison purposes with SMA. The MSEcr is utilized in the first stage to predict the location of the damaged elements. Single and multiple damages cases are analysed based on different number of modes to study the sensitivity of the proposed indicator to the total number of modes considered in the analysis. Next, this indicator is used as an objective function in a second stage to solve the inverse problem using SMA and MPA for damage quantification of the elements identified in the first stage. Experimental validation is conducted using a 3D frame structure with four stories that have damaged components. It is demonstrated that the proposed approach, using MSEcr and SMA, provides superior results for the considered structures. The effectiveness of this technique is tested by introducing a white Gaussian noise with different levels, namely 2% and 4%. The results show that the provided approach can predict the location and level of damage with high accuracy after introducing the noise.

Keywords Modal strain energy · Damage indicator · Slime mould algorithm · Marine predators algorithm · Inverse problem · Modal analysis · Damage assessment

✉ Magd Abdel Wahab
magd.abdelwahab@tdtu.edu.vn

Samir Tiachacht
Samir.tiachacht@ummto.dz

Samir Khatir
Khatir_samir@hotmail.fr

Cuong Le Thanh
Cuong.lt@ou.edu.vn

Ravipudi Venkata Rao
Ravipudirao@gmail.com

Seyedali Mirjalili
Ali.mirjalili@gmail.com

1 Laboratory of Mechanics, Structure and Energetics (LMSE), Mouloud Mammeri University of Tizi-Ouzou, B.P. N° 17 RP, 15000 Tizi Ouzou, Algeria

2 Soete Laboratory, Faculty of Engineering and Architecture, Ghent University, Technologiepark Zwijnaarde 903, 9052 Zwijnaarde, Belgium

3 Faculty of Civil Engineering, Ho Chi Minh City Open University, Ho Chi Minh City, Vietnam

4 Department of Mechanical Engineering, Sardar Vallabhbhai National Institute of Technology, Surat, Gujarat, India

5 Centre for Artificial Intelligence Research and Optimisation, Torrens University Australia, Fortitude Valley, Brisbane, QLD 4006, Australia

6 Yonsei Frontier Lab, Yonsei University, Seoul, Korea

7 Division of Computational Mechanics, Ton Duc Thang University, Ho Chi Minh City, Vietnam

8 Faculty of Civil Engineering, Ton Duc Thang University, Ho Chi Minh City, Vietnam

1 Introduction

In all civil structure such as bridges, the protection of offshore and buildings is an important matter. Data focused on vibration analysis have gained considerable attention in the last 3 decades. A variety of approaches based on modal analysis was proposed in [1, 2] to predict the existing of damage. The most recent analysis of damage was focused on using modal curvature and damage indicators, which were based on healthy and unhealthy structures as mentioned in [3]. Rytter [4] suggested a comparison of various techniques based on four levels: (a) existing of damage, (b) position of damage, (c) potential of damage and (d) remaining life. Yang and Liu [5] used residual force vector (RFV) to predict the damaged elements. Three damages scenarios were considered to test the ability of this technique for a plane truss structure. Furthermore, different noise levels were introduced to test the effectiveness of these techniques. The damage localization was impossible when the measured mode shape had a large measurement noise. The modified Cornwell indicator (MCI) was improved by Tiachacht et al. [6] for solving damage identification in complex structures. The provided results showed that MCI was more accurate than CI in single and multiple damages. In the second stage, the authors used MCI as an objective function to estimate the potential of damage correctly.

Static and dynamic analyses of the damaged RC beams were developed by Capozucca [7] based on an experimental study. The beams were strengthened with near-surface mounted (NSM) carbon fibre reinforced polymer (CFRP) rods based on experimental analysis. Cha and Buyukozturk [8] performed structural health monitoring (SHM) based on mode shapes using modal strain energy indicator (MSEI) combined with hybrid multi-objective genetic algorithm (GA) for various three-dimensional steel structures. The investigated method could detect correctly the position and level of damaged elements. Khatir et al. [9, 10] used different optimization techniques for solving an inverse problem to predict the location and the potential of damaged elements in composite beams. The objective function was based on frequencies and mode shapes. Single and multiple damages scenarios were considered to test the accuracy of the proposed approaches. The obtained results showed that the provided approaches could detect correctly the position and level of damage. Nobahari et al. [11] presented an efficient approach for multiple damages for simple and complex structures. The approach introduced a flexibility strain energy-based index (FSEBI). The provided results showed that the proposed technique could detect correctly the position of the damage. Pandey et al. [12] provided an approach for damage identification based on the change in the structure flexibility matrix. This technique can detect and locate correctly the damaged elements and was validated using experimental data. Three-dimensional frame structures were analysed using numerical methods for damage identification using genetic algorithm (GA) as an inverse problem in [13]. Natural frequencies were used as an objective function to compare the measured and calculated values. GA could predict the single damage after few iterations and more than 80 iterations for multiple damage.

Khatir et al. [14] presented an approach based on model reduction for crack identification in CFRP composite beam. The data were extracted from experimental analysis based on different crack configurations, i.e. position, depth and width. The provided results were more accurate compared with FEM and analytical solution. Zenzen et al. [15] presented a modified damage indicator based on transmissibility and mode shapes for a laminated composite beam and plate. The provided indicator can predict the position and level of damage correctly. Furthermore, machine learning using ANN was used for damage quantification after collecting the data based on damage index as input and reduction in stiffness as output. FRF damage indicator was proposed by Hwang and Kim [16] to predict the position and level of damaged beam-like structures. The FRF was used as an objective function with optimization technique in [17]. The results were good enough to predict correctly the damaged elements. Different applications were provided in the literature to predict the existence of damage in various types of structures.

Two techniques based on the changes in the mode shapes and mode-shape-slope parameters were investigated by Yuen [18]. Yang [19] used modal residual force (MRF) criteria and matrix disassembly technique for structural damage identification. Multiverse optimizer (MVO) is used to solve damage identification problem by Ghannadi et al. [20]. Two objective functions were used to solve the inverse problem based on the modal assurance criterion (MAC) and modified total modal assurance criterion (MTMAC). Grey wolf optimizer (GWO) was used for SHM of frame structures by Ghannadi et al. [21]. Natural frequencies and mode shapes were considered as an objective function to compare the measured and calculated values. A fixed free beam and a truss tower based on experimental modal analysis were used to validate the proposed approach. The provided results were accurate for different kind of structures. Khatir et al. [9, 22–25] used different optimization techniques for damage identification based on inverse problem using different kinds of structures such as steel and composite beams and plates, and complex structures. Ghannadi and Kourehli [26–29] presented different techniques for structural health monitoring based on inverse problem and machine learning.

This paper presents a damage detection, localization and quantification using modal strain energy change ratio (MSEcr) as damage indicator combined with a new optimization technique, namely slime mould algorithm (SMA) developed in 2020 for fast prediction. The SMA algorithm is employed to assess structural damage and monitor structural health. Two kinds of structures, including a laboratory beam and a bar planar truss, are considered to study the effectiveness of the proposed approach. Another recent algorithm called marine predators algorithm (MPA) is also used for comparison purposes with SMA.

2 Theoretical background

In this section, the preliminaries and essential definitions required for this work are given.

2.1 Modal strain energy change ratio

The reduction of stiffness with nel number of elements and damage parameter $\delta_i\,(i = 1, 2, \ldots, \mathrm{nel})$ is presented in the following equation:

$$K_{\mathrm{d}} = \sum_{i=1}^{\mathrm{nel}} \left(1 - \delta_i\right) k_i^e, \tag{1}$$

where K_{d} is the damaged stiffness matrix, k_i^e is the stiffness matrix of the ith element and δ_i is a damage parameter having a value between 0 and 1; i.e. 0 for intact and 1 is fully damaged structure.

The modal strain energy (MSE) for undamaged and damaged structures are presented in the following formulation:

$$\mathrm{MSE}_{ij}^{h} = \frac{1}{2}\left(\phi_i^h\right)^T K_j\, \phi_i^h\,; \quad \mathrm{MSE}_{ij}^{d} = \frac{1}{2}\left(\phi_i^d\right)^T K_j\, \phi_i^d, \tag{2}$$

where, ith is the mode number and jth is the element number. The superscript T denotes the vector transpose, ϕ_i is mode shape, h and d denote the healthy and damaged systems, respectively, and K_j presents the stiffness matrix. The modal strain energy change ratio (MSEcr) is proposed to predict the exact location of the damage. (MSEcr) can be written using the total energy in the structure, which may be determined by the addition of the MSE's of all elements as follows:

$$\mathrm{MSEcr}_j = \frac{1}{m} \sum_{j=1}^{m} \frac{\mathrm{MSEcr}_{ij}}{\mathrm{MSEcr}_{ij}^{\max}}, \tag{3}$$

where

$$\mathrm{MSEcr}_{ij} = \frac{\left|\mathrm{MSE}_{ij}^{d} - \mathrm{MSE}_{ij}^{h}\right|}{\mathrm{MSE}_{ij}^{h}}\;; \quad \mathrm{MSEcr}_{ij}^{\max} = \max_k \left\{\mathrm{MSEcr}_{ik}\right\}. \tag{4}$$

2.2 Description of slime mould algorithm

SMA is a new algorithm introduced recently by Li et al. [30]. The concept of this optimisation technique is based on the behaviour and morphological changes of slime mould in nature. At the same moment, the use of weights in SMA is a brand new concept to model the positive and negative feedback provided by slime moulds through foraging, thus producing three distinct morphotypes. In this paper, structural damage identification is analysed based on inverse problem using SMA. The following mathematical formula describes the advancing behaviour of the slime mould:

$$\overrightarrow{X(t+1)} = \begin{cases} \overrightarrow{X_b(t)} + \overrightarrow{vb} \cdot \left(\overrightarrow{W} \cdot \overrightarrow{X_A(t)} - \overrightarrow{X_B(t)}\right), & r < p \\ \overrightarrow{vc} \cdot \overrightarrow{X(t)} & r \geq p \end{cases}, \tag{5}$$

where $\overrightarrow{vb}$ denotes a parameter with a range of $[-a, a]$, t denotes the current iteration, $\overrightarrow{X_b}$ presents the individual position with the highest odour concentration currently found, $\overrightarrow{vc}$ is a parameter that decreases linearly from 1 to 0, $\overrightarrow{X}$ denotes the location of slime mould. Two individuals are chosen randomly from the swarm, i.e. $\overrightarrow{X_A}$ and $\overrightarrow{X_B}$, and $\overrightarrow{W}$ is the weight of slime mould.

The parameter p is described as follows:

$$\begin{gathered} p = \tanh\left|S(i) - DF\right|, \\ (i \in 1, 2, \ldots, n), S(i) \text{ is the fitness of } \vec{X}, \end{gathered} \tag{6}$$

where DF denotes the best fitness obtained in all iterations.

The parameter $\overrightarrow{vb}$ is written as follows:

$$\overrightarrow{vb} = [-a, a], \tag{7}$$

$$a = \operatorname{arctanh}\left(-\left(\frac{t}{\max\_t}\right) + 1\right), \tag{8}$$

where $\overrightarrow{W}$ is described in the following formulation:

$$\overrightarrow{W(\text{Smell Index}(i))} = \begin{cases} 1 + r \cdot \log\left(\frac{bF - S(i)}{bF - wF} + 1\right), & \text{condition} \\ 1 - r \cdot \log\left(\frac{bF - S(i)}{bF - wF} + 1\right), & \text{other} \end{cases}, \tag{9}$$

$$\text{Smell Index} = \operatorname{sort}(S), \tag{10}$$

where 'condition' signifies that $S(i)$ ranks first half of the population, r means the random value between $[0, 1]$, In the current iterative process, bF indicates the optimum fitness achieved, wF signifies the worst fitness value previously achieved in the iterative process, Smell Index evaluates the

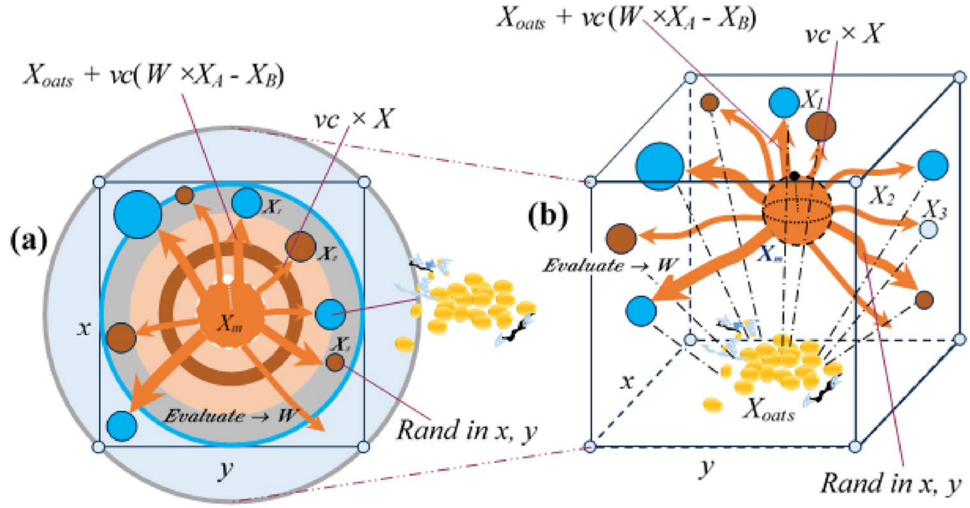

Fig. 1 Possible locations in 2D and 3D [30]

sequence of fitness values listed. Figure 1 demonstrates the process of possible locations in 2D and 3D.

Updating the location of slime mould can be explained by the following mathematical formulas:

$$\overrightarrow{X^*} = \begin{cases} \text{rand} \cdot (UB - LB) + LB & \text{rand} < z \\ \overrightarrow{X_b(t)} + \overrightarrow{vb} \cdot \left(W \cdot \overrightarrow{X_A(t)} - \overrightarrow{X_B(t)} \right) & r < p \\ \overrightarrow{vc} \cdot \overrightarrow{X(t)} & r \geq p \\ \text{LB and UB are lower and upper boundaries} \end{cases} . \quad (11)$$

The value of $\overrightarrow{vb}$ oscillates randomly between $[-a, a]$ when the iterations rise, it reaches zero steadily. For more details, the following pseudo-code describes the methodology of SAM.

2.3 Description of marine predators algorithm

This section describes MPA [31], which is a population-based approach similar to most metaheuristics algorithms. During these algorithms, the initial solution is spread with the first analysis uniformly over the problem space, i.e.:

$$X_0 = X_{\min} + \text{rand}\left(X_{\max} - X_{\min}\right), \quad (12)$$

where $X_{\min}$ and $X_{\max}$ significate the lower and upper bound, respectively, for variables, and *rand* denotes a random vector [0, 1].

Top predators in nature are more proficient in finding food, based on the survival of the fittest principle. The fittest solution is, therefore, nominated to create a matrix called

Algorithm 1 Pseudo-code of SMA

Initialization the parameters $\left(population\,size, Max\_iteration\right)$
Initialization the positions of slime mould $X_i\left(i = 1, 2, \ldots, n\right)$;
While $\left(t \leq Max\_iteration\right)$
  Calculate the fitness of all slime mould;
  $Update\,bestFitness,\ X_b$
  $Compute\,the\,W$;
  For $each\,search\,position$;
    $Update\ p, vb, vc$;
    $Update\ positions$;
  End For
  $t = t + 1$;
End While
Return $bestFitness,\ X_b$;

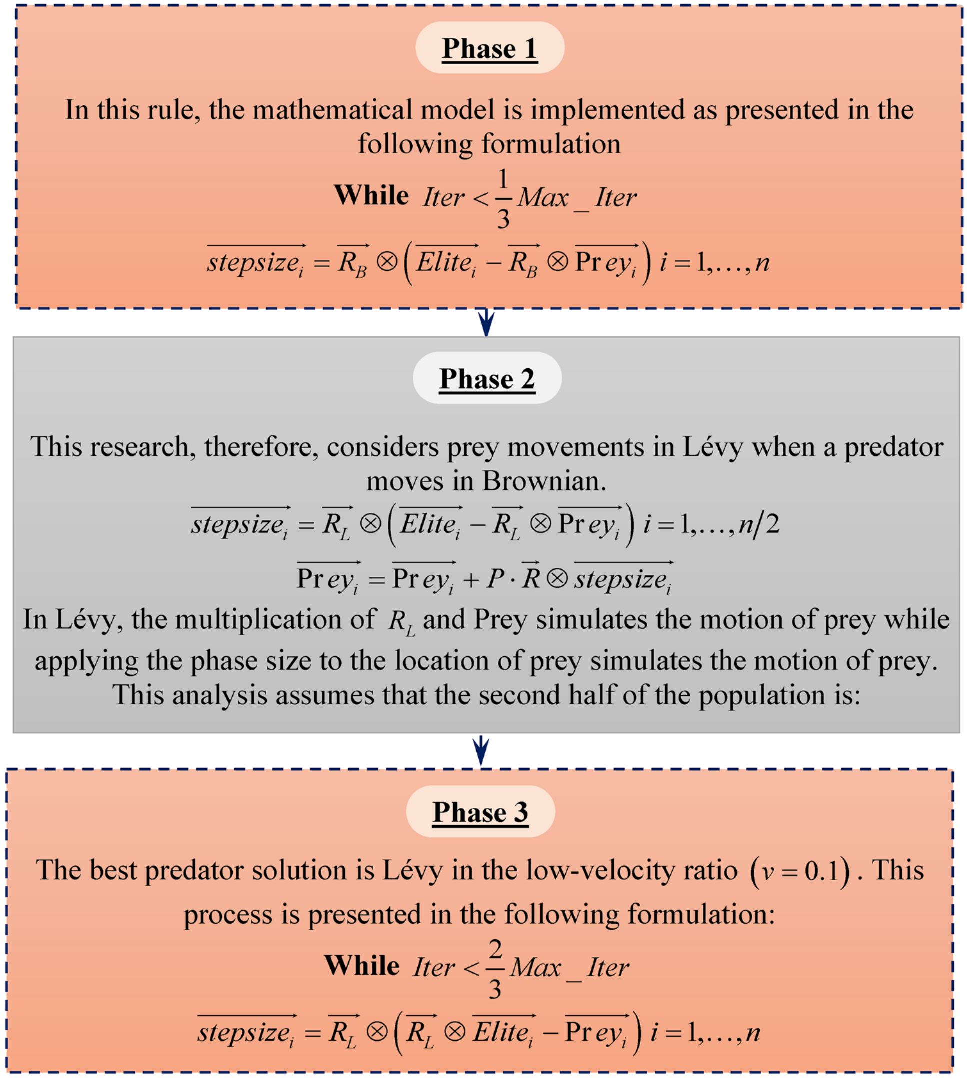

Fig. 2 Flowchart describe the three phases of MPA [31]

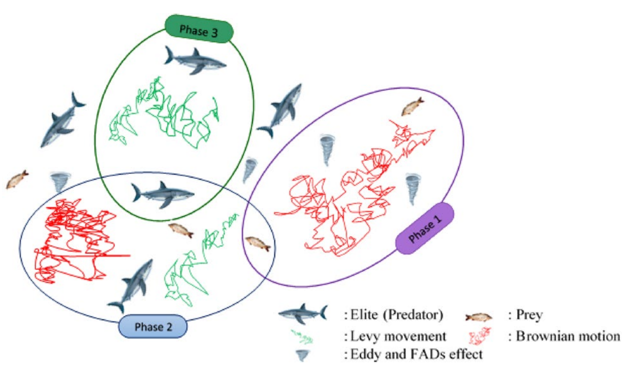

Fig. 3 The three MPA optimization phases [31]

Elite as a top predator. Depending on the information on prey locations, arrays of this matrix supervise the search and finding of the prey.

$$\text{Elite} = \begin{bmatrix} X^I_{1,1} & X^I_{1,2} & \cdots & X^I_{1,d} \\ X^I_{2,1} & X^I_{2,2} & \cdots & X^I_{2,d} \\ \vdots & \vdots & \ddots & \vdots \\ X^I_{n,1} & X^I_{n,2} & \cdots & X^I_{n,d} \end{bmatrix}_{n \times d}, \tag{13}$$

where X^I is the top predator vector and n denotes the number of search agents, while d is the number of dimensions. Prey is another matrix of the same dimension as Elite, and the predators change their positions based on it as follows:

$$\text{Prey} = \begin{bmatrix} X_{1,1} & X_{1,2} & \cdots & X_{1,d} \\ X_{2,1} & X_{2,2} & \cdots & X_{2,d} \\ X_{3,1} & X_{3,2} & \cdots & X_{3,d} \\ \vdots & \vdots & \ddots & \vdots \\ X_{n,1} & X_{n,2} & \cdots & X_{n,d} \end{bmatrix}_{n \times d}, \tag{14}$$

where $X_{i,j}$ denotes the jth dimension of ith prey.

The process of MPA consists of three major optimization stages, taking into account various velocity ratios and simultaneously mimicking the entire life of a predator and prey such as:

1. With a high velocity ratio or when the prey runs faster than the predator.
2. Unit velocity ratio or when both predator and prey travel at approximately the same rate.
3. When the predator runs faster than the prey, at a low velocity ratio.

These phases are described based on the rules regulating the movement of predators and prey while mimicking the movement of predators and prey in nature. These three steps are demonstrated in the flowchart shown in Fig. 2.

The three stages of optimization are displayed graphically in Fig. 3. First, in phase 1 of optimization, in Brownian motion, prey moves. When these preys are distributed equally in the search domain in the first iterations and the gap around predator and prey is significantly higher, Brownian motion will enable preys to explore their neighbourhood separately, due to the good exploration of the domain.

3 Damage detection using MSEcr

In this section, two structures are considered, namely a simply supported laboratory beam and 31 bar planar truss, to investigate the effectiveness and the accuracy of the damage indicator MSEcr.

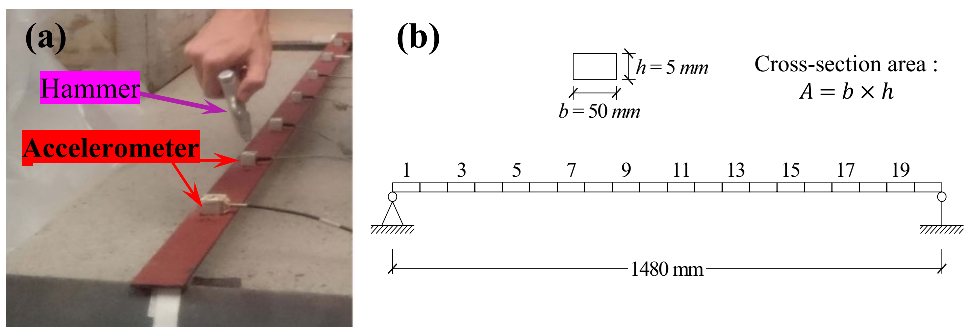

Fig. 4 **a** Experimental beam and **b** configurations and boundary conditions [32]

Table 1 Comparison between numerical and experimental natural frequencies of healthy and damaged beams

Mode	Experiment [32] (Hz)-healthy	FEM (Hz)-healthy	Error (%)	Natural frequency (Hz)					
				Damaged-case 1	Error (%)	Damaged-case 2	Error (%)	Damaged-case 3	Error (%)
1	5.10	5.08	0.22	5.07	0.61	5.02	1.4	5	1.7
2	20.01	20.35	1.71	20.18	0.85	20.17	0.80	20.02	0.07

Error is presented as an absolute value

Table 2 Reduction in stiffness for each damage case

Case 1		Case 2		Case 3	
Element no	Damage rate (%)	Element no	Damage rate (%)	Element no	Damage rate (%)
5	15	4	10	3	20
–	–	10	15	7	10
–	–	17	10	8	5
–	–	–	–	11	10
–	–	–	–	18	15

Fig. 5 Damage detection—a simply supported beam—case 1

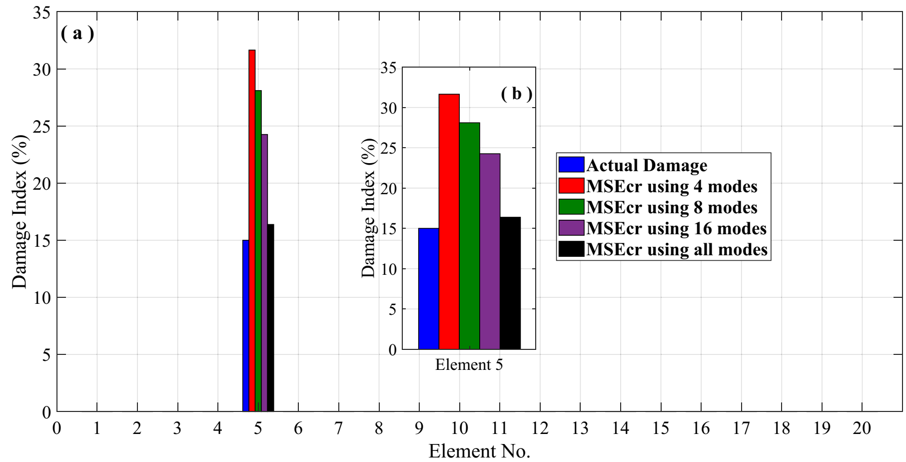

Fig. 6 Damage detection—a simply supported beam—case 2

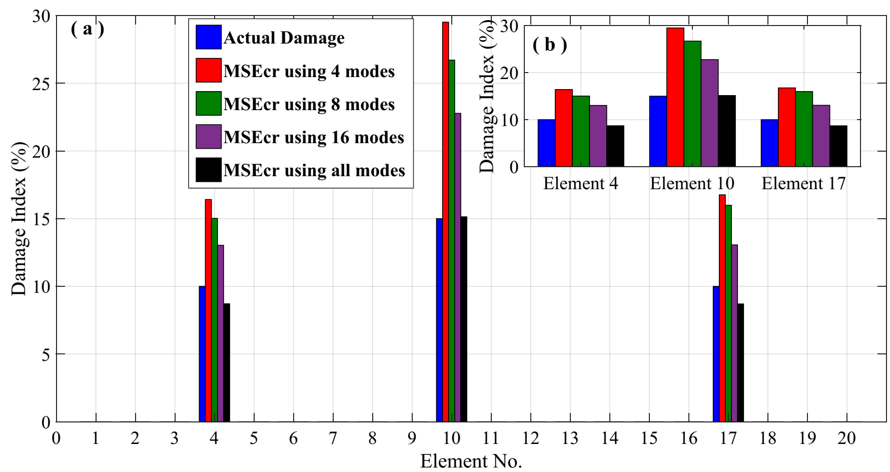

Fig. 7 Damage detection—a simply supported beam—case 3

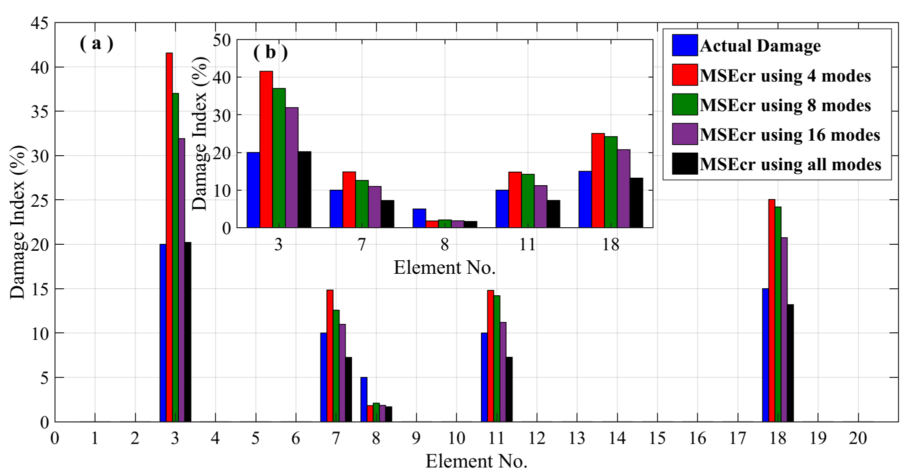

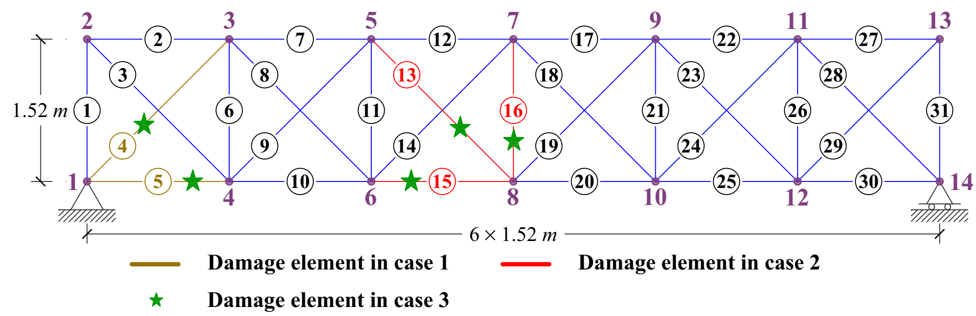

Fig. 8 A FEM for a 31-bar planar truss

Table 3 Percentage of stiffness reduction of simply supported beam elements

Case 4		Case 5		Case 6	
Element no	Damage rate (%)	Element no	Damage rate (%)	Element no	Damage rate (%)
4	10	13	15	4	10
5	15	15	10	5	15
–	–	16	15	13	15
–	–	–	–	15	10
–	–	–	–	16	15

Table 4 Natural frequencies of a 31-bar planar truss

Mode	FEM [33]	FEM (Hz)	Error (%)	Natural frequency (Hz)					
				Damaged-case 4	Error (%)	Damaged-case 5	Error (%)	Damaged-case 6	Error (%)
1	36.09	36.168	0.22	35.986	0.29	35.850	0.66	35.671	1.16
2	75.63	75.544	0.11	73.184	3.23	75.338	0.39	73.014	3.46
3	132.95	132.841	0.08	132.087	0.65	132.185	0.58	131.442	1.13
4	220.95	221.762	0.37	218.435	1.14	219.820	0.51	216.504	2.01

Please note that error is presented as absolute value

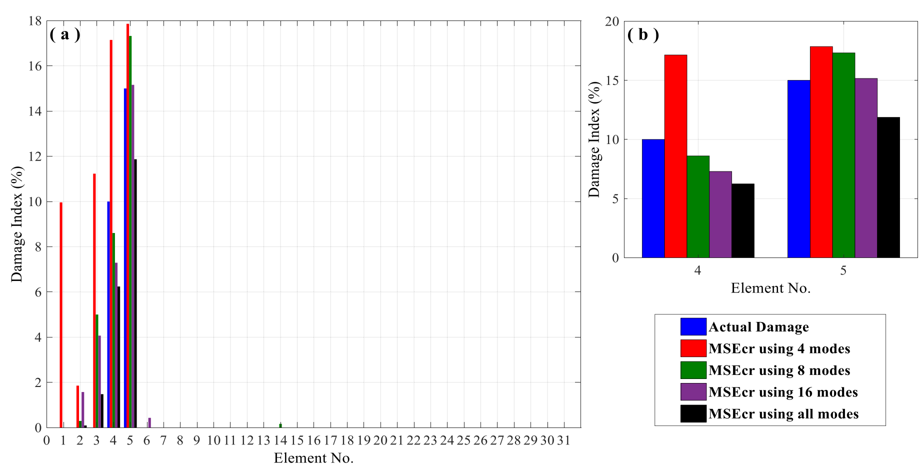

Fig. 9 Damage detection—a 31-bar planar truss—case 4

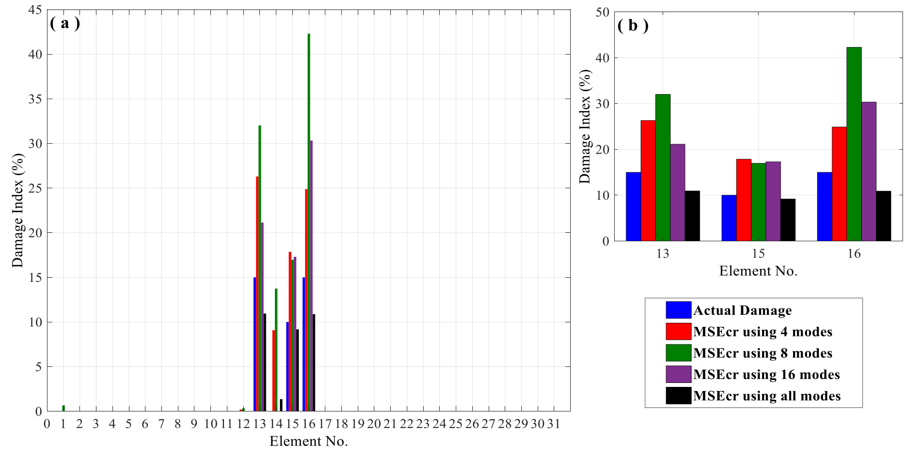

Fig. 10 Damage detection—a 31-bar planar truss—case 5

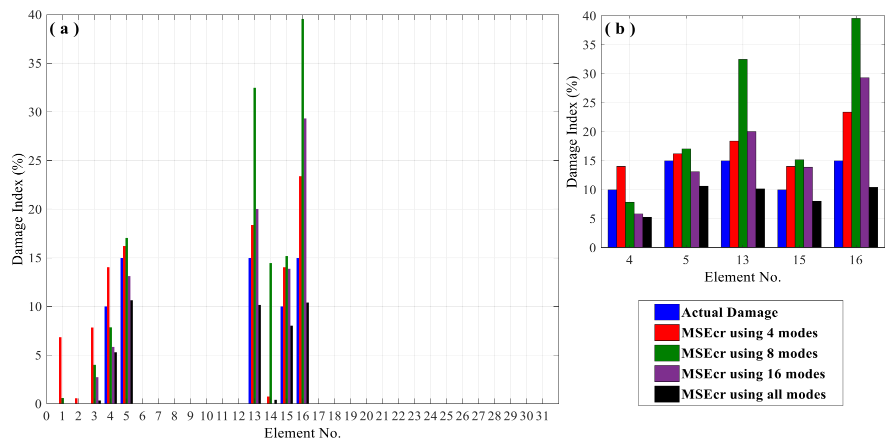

Fig. 11 Damage detection—a 31-bar planar truss—case 6

3.1 A laboratory beam

First, a simply supported steel beam with rectangular cross-section discretised in 20 elements is used with the mechanical properties of $E = 200$ GPa and $\rho = 7850\ \mathrm{kg/m^3}$ and geometrical properties $(L \times b \times h) = 1480 \times 50 \times 5\ \mathrm{mm^3}$ as shown in Fig. 4 [32]. The frequencies are presented in Table 1 for healthy and damaged beams.

Three cases are analysed to test the accuracy of the presented indicator based on multiple and single damages as listed in Table 2.

Three cases are considered based on multiple damages to study the effectiveness of MSEcr using different numbers of modes, e.g. 4, 8, 16 and all of them. The results are provided for each case in Figs. 5, 6 and 7.

Based on the presented results, MSEcr can predict correctly the location of damaged elements using different numbers of modes. The objective to study the effect of number of modes is to predict location of damaged elements and the speed of convergence, when SMA and MPA are used for damage quantification in Sect. 4.

3.2 A 31-bar planar truss

A simply supported plane truss structure has 31 aluminium alloy bars with 9.12 m total length, 1.52 m height and 0.0025 m^2 cross-sectional area. A finite element (FE) model of the truss structure was built in MATLAB software. One element is used to simulate each bar of the truss structure and the total number of nodes are 14 as shown in Fig. 8. The mechanical properties are: Young modulus's $E = 70$ GPa and density $\rho = 2770\ \mathrm{kg/m^3}$. Three scenarios are introduced to the 31-bar planar truss based on single and multiple damages as illustrated in Table 3. The presented structure is simply supported at nodes 1 and 14. The first five natural

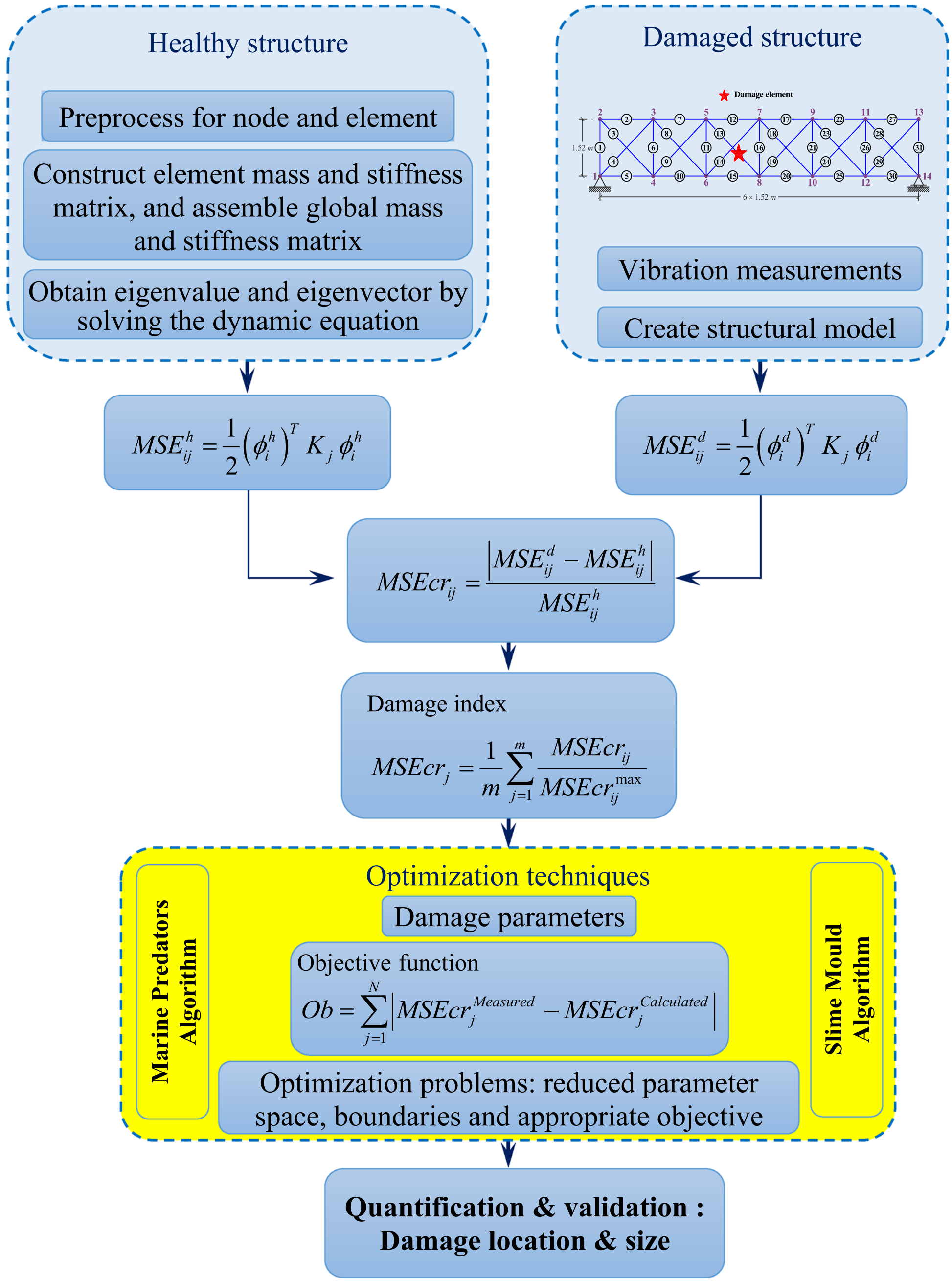

Fig. 12 Flowchart for MPA and SMA using MSEcr

frequencies are listed in Table 4 for the healthy beam and damaged for cases 4–6.

Three damage cases are investigated for the 31-bar planer truss based on single and multiple damages to analyse the performance of *MSEcr* in 2D structure using different numbers of modes 4, 8, 16 and all of them. The results are shown for each case in Figs. 9, 10 and 11.

Based on Figs. 9, 10 and 11, it can be seen that MSEcr predicts correctly the exact location of damaged elements using different number of modes. Prediction with less number of modes is analysed to estimate the position of damaged elements. In addition, the quantification will be predicted using SMA and MPA in the next section.

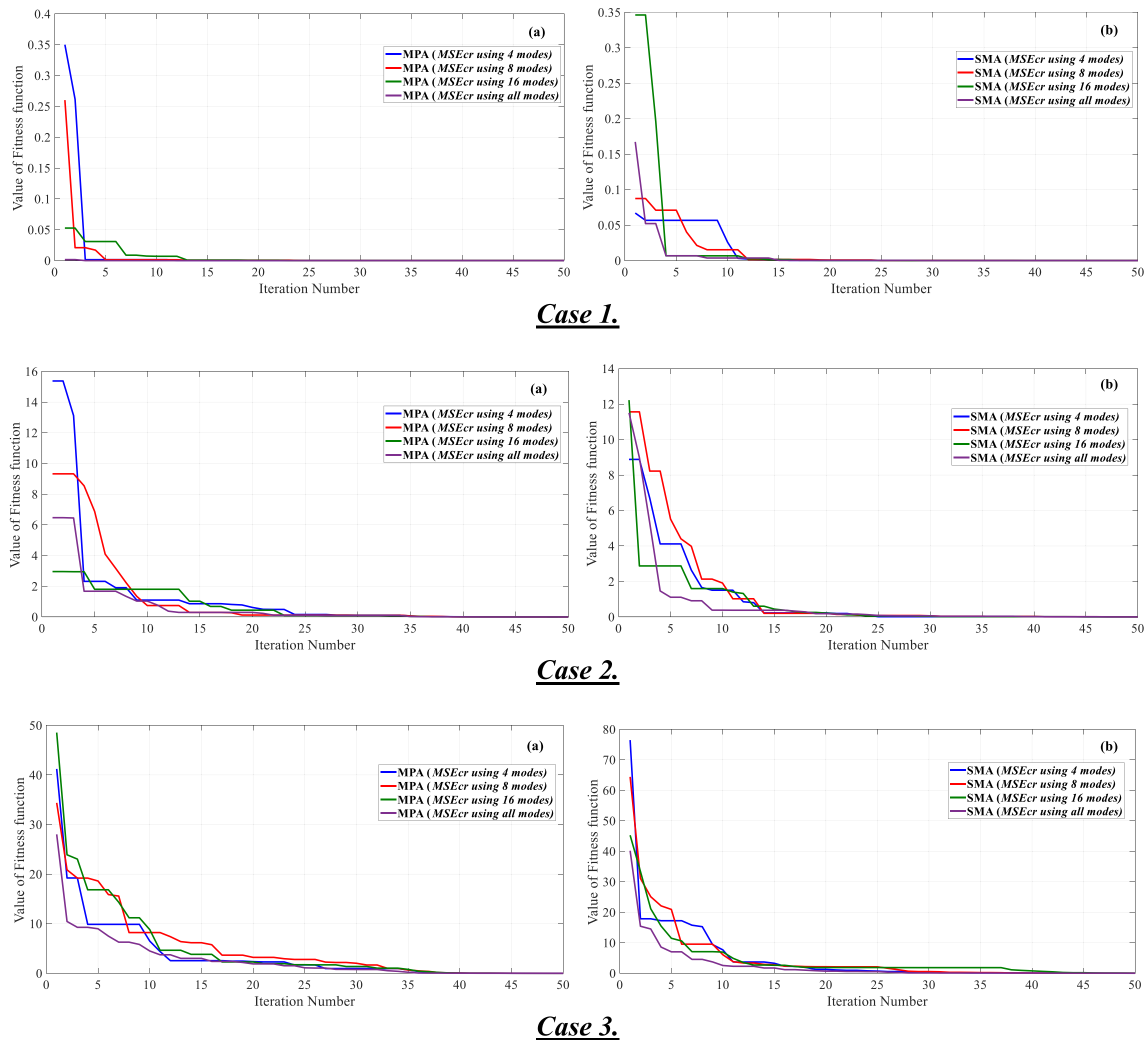

Fig. 13 A simply supported beam: convergence of fitness function of all cases—SMA (right) and MPA (left)

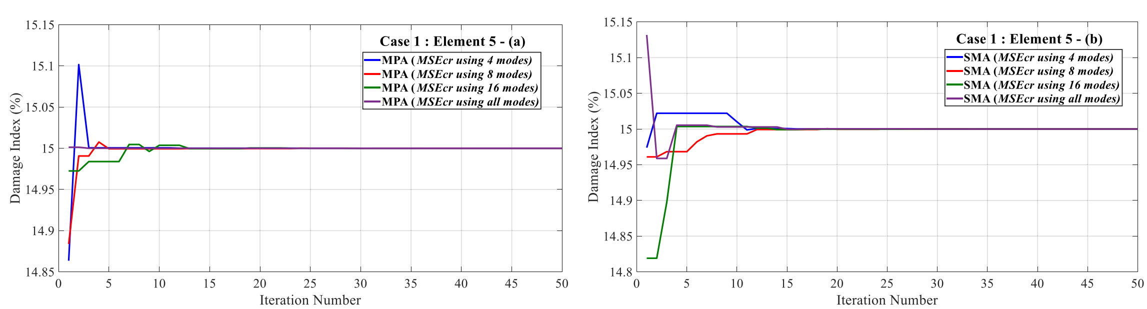

Fig. 14 A convergence study of simply supported laboratory beam—case 1

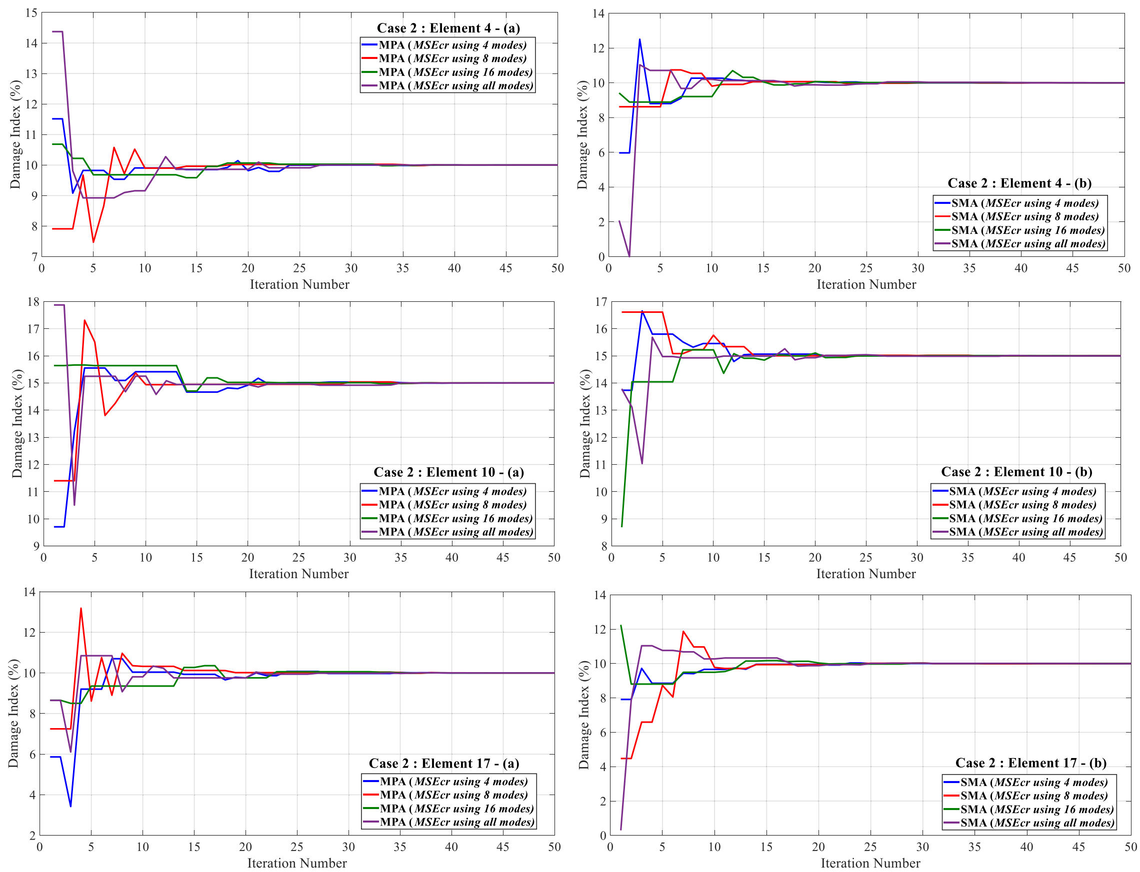

Fig. 15 A convergence study of simply supported laboratory beam—case 2

4 Damage quantification

Based on the previous section, the damaged elements are predicted correctly using MSEcr. However, the damage quantification will be presented in this section for all scenarios in both considered structures. Both SMA and MPA are used to solve damage quantification based on one parameter after detecting the location using the damage indicator, MSEcr. Fifty generations and 100 populations are selected to solve the optimization process problem for both algorithms. Figure 12 describes the inverse problem using MPA and SMA using MSEcr as an objective function.

4.1 Objective function

MSEcr is used as an objective function for damage quantification to make a comparison between measured and calculated values as follows:

$$\text{Ob} = \sum_{j=1}^{N} \left| \text{MSEcr}_j^{\text{Measured}} - \text{MSEcr}_j^{\text{Calculated}} \right|, \tag{15}$$

where $\text{MSEcr}_j^{\text{Measured}}$ presents the measured damage index and $\text{MSEcr}_j^{\text{Calculated}}$ presents the damage index of damaged elements calculated during the process of the optimisation using SMA and MPA.

4.2 A laboratory beam

The convergence of objective function (fitness) for each scenario is presented in Fig. 13, and the convergence of damaged element using SMA and MPA is presented in Figs. 14, 15 and 16. The presented results are based on the used number of modes. The fitness values for different iterations and different numbers of modes using SMA and MPA are summarized in Table 5 for the laboratory beam.

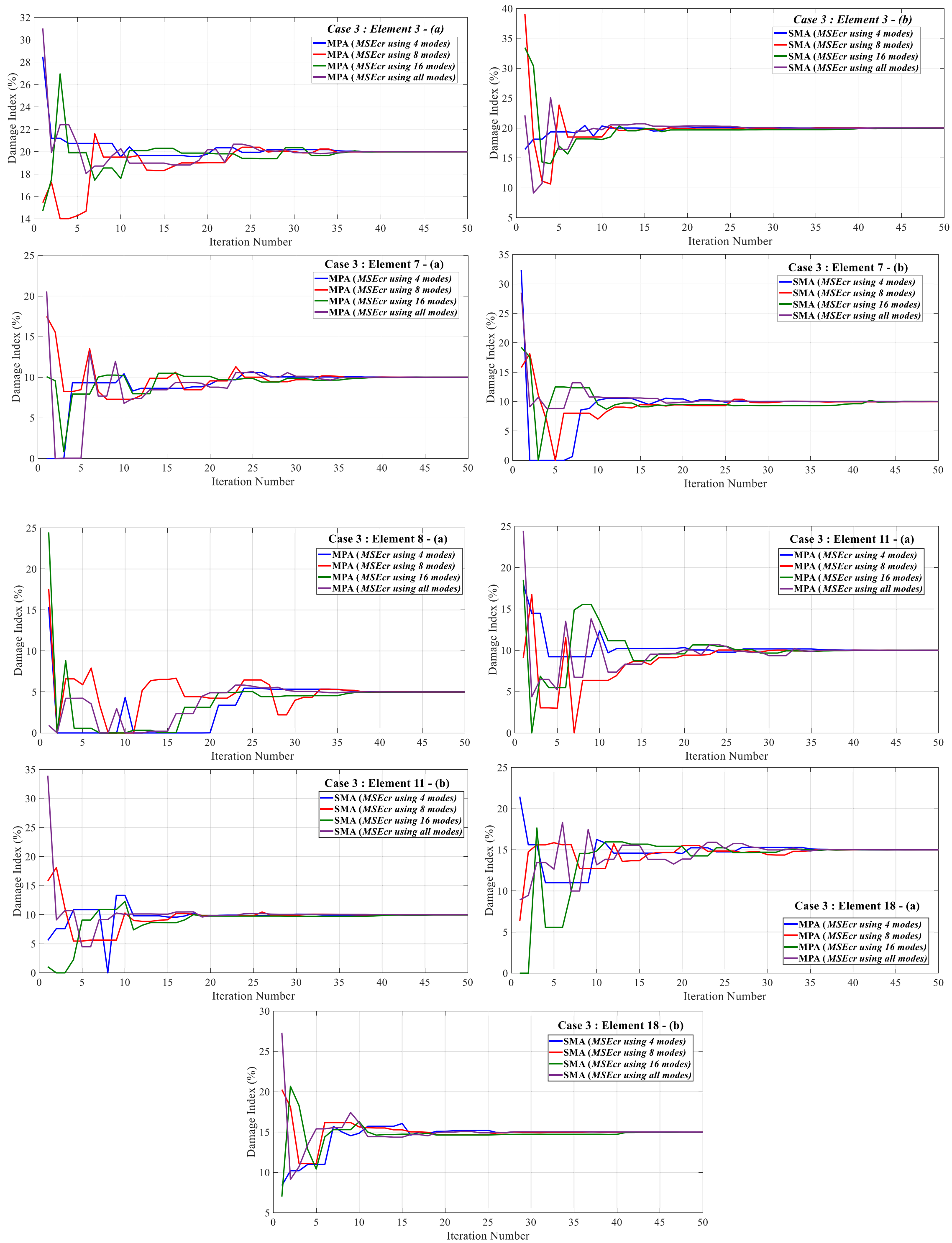

Fig. 16 A convergence study of simply supported laboratory beam—case 3

The first damage case is predicted after few iterations using both algorithms for different numbers of modes. For Case 2, the results can be predicted after 25 iterations for SMA and 35 for MPA, and for the last case using five damaged elements SMA can predict the results after 20 iterations and MPA after 35. Table 6 presents the details of computational time taken for analysing the simply supported laboratory beam for different numbers of modes.

Table 5 Fitness values for different iterations and different numbers of modes for the simply supported laboratory beam using SMA and MPA

Case	Number of mode	Optimization method	Iteration					
			1	10	20	30	40	50
1	4	MPA	0.35	0.0015	0.000258	0.0000176	0.0000176	0.000000406
		SMA	0.067	0.0259	0.000333	0.000192	0.0000418	0.0000185
	8	MPA	0.26	0.00142	0.000725	0.0000469	0.000000306	0.000000306
		SMA	0.0875	0.0153	0.000907	0.000177	0.0000221	0.0000039
	16	MPA	0.0528	0.00699	0.000581	0.0000242	0.00000456	0.000000661
		SMA	0.346	0.00673	0.000256	0.0000163	0.0000163	0.0000124
	All	MPA	0.00161	0.00000835	0.00000835	0.00000504	0.00000108	0.000000169
		SMA	0.167	0.00365	0.000354	0.000057	0.0000501	0.00000232
2	4	MPA	15.4	1.1	0.617	0.113	0.00932	0.0000636
		SMA	8.88	1.51	0.228	0.0132	0.0132	0.00355
	8	MPA	9.32	0.743	0.124	0.114	0.0049	0.0000438
		SMA	11.6	1.91	0.204	0.0641	0.0291	0.00444
	16	MPA	2.96	1.8	0.441	0.103	0.00292	0.000119
		SMA	12.2	1.6	0.218	0.0385	0.0128	0.00203
	All	MPA	6.47	1.03	0.295	0.102	0.00486	0.0000532
		SMA	11.5	0.383	0.185	0.0647	0.019	0.00403
3	4	MPA	41.2	6.49	2.35	0.953	0.0525	0.00115
		SMA	76.5	7.67	1.26	0.29	0.0824	0.0169
	8	MPA	34.4	8.21	3.2	2.02	0.0473	0.00169
		SMA	64.4	6.07	2.15	0.555	0.0794	0.0244
	16	MPA	48.5	8.81	2.28	1.37	0.0337	0.000627
		SMA	45.3	6.95	1.88	1.85	0.786	0.0521
	All	MPA	28	4.5	1.89	0.761	0.0135	0.000381
		SMA	40.2	2.55	0.692	0.0997	0.0659	0.0108

Table 6 CPU time (s) for the simply supported laboratory beam

Number of modes	CPU time (s)					
	Case 1		Case 2		Case 3	
	MPA	SMA	MPA	SMA	MPA	SMA
4	81.850142	41.151385	79.681453	42.876808	80.583801	42.497276
8	97.353196	49.820114	98.729919	50.016257	97.189691	48.983169
16	129.049458	66.315400	131.588686	65.055388	131.876821	65.233786
All	227.553167	113.670628	227.972770	112.880179	222.430493	116.339493

4.3 A 31-bar planar truss

The convergence of the objective function (fitness) for each scenario of the 31-bar planar Truss is plotted in Fig. 17, whereas the convergence of damaged elements is presented in Figs. 18, 19 and 20 using different numbers of mode.

The fitness values for different iterations and different numbers of modes are summarized in Table 7 for the 31-bar planar truss.

Based on the convergence of damaged elements, case 4 can be predicted after 10 iterations using SMA and 20 using MPA for different numbers of modes. For Case 5, the best convergence is achieved after 14 iterations for SMA compared with 25 iterations for MPA, and for case 6, SMA can predict the results correctly after 17 iterations compared with 35 iterations for MPA. Table 8

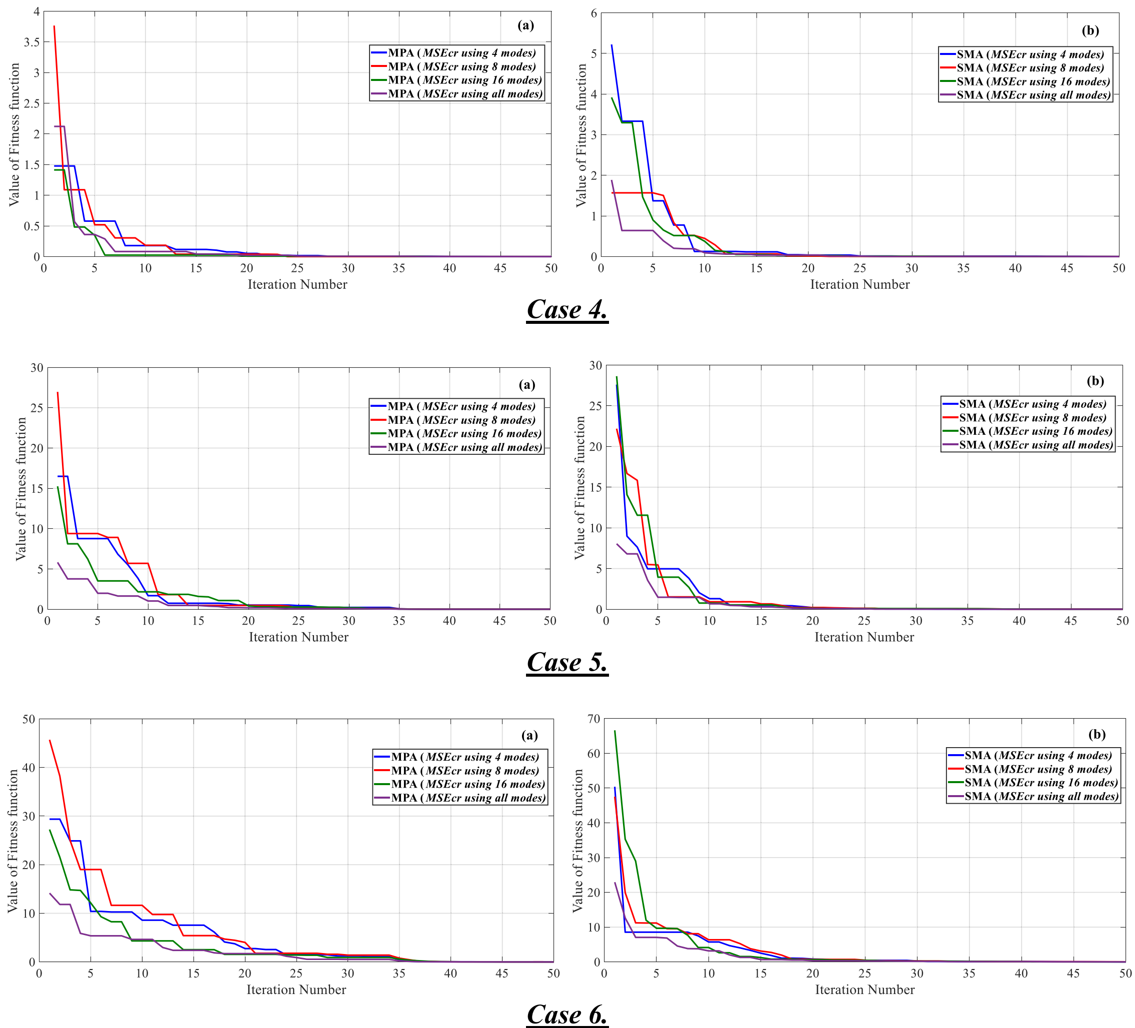

Fig. 17 A 31-bar planar truss: convergence of fitness function for all cases—SMA (right) and MPA (left)

presents details of computational time taken for analysing the 31 bar planar truss for different numbers of modes.

The provided results show that SMA has good convergence compared with MPA for different scenarios and structures. Moreover, SMA requires less CPU time compared with MPA.

5 Experimental validation

In this section, experimental tests of a four-story steel frame are used for validation of the proposed method, as illustrated in Fig. 21. This frame was examined in New York at Columbia University. The same measurements were analysed for damage detection using different techniques in [21, 34]. A hydraulic shake table was used to excite the frame structure as illustrated in the bottom of Fig. 18. Piezoelectric accelerometers were used to measure the structural responses. The positions of the sensors are shown in Fig. 21. For the geometrical properties, the inter-story height is 533 mm, column cross-sectional dimensions are 50.8×9.5 mm^2 and dimensions of floor plate are $610 \times 457 \times 12.7$ mm^3. The structural elements are attached to bolts, enabling members to be easily replaced and modified. The cross-section of one column between the second and third floors was reduced and can be expressed by 66% level of damage as shown in Fig. 21.

The natural frequencies are listed in Table 9 for the healthy and damaged steel frames. The natural frequencies

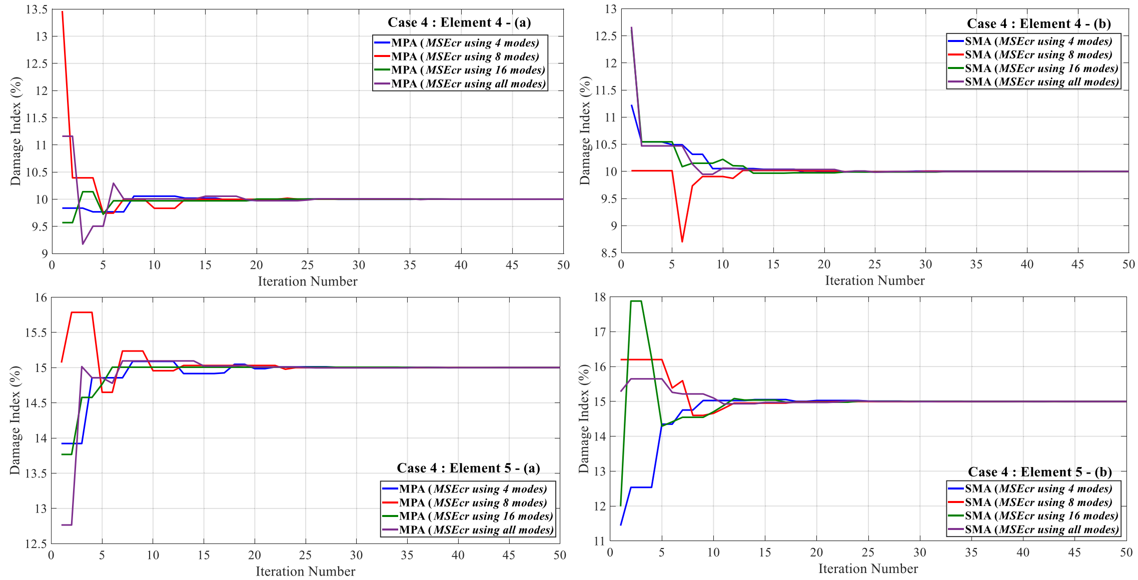

Fig. 18 A convergence study of 31-bar planar Truss—case 4

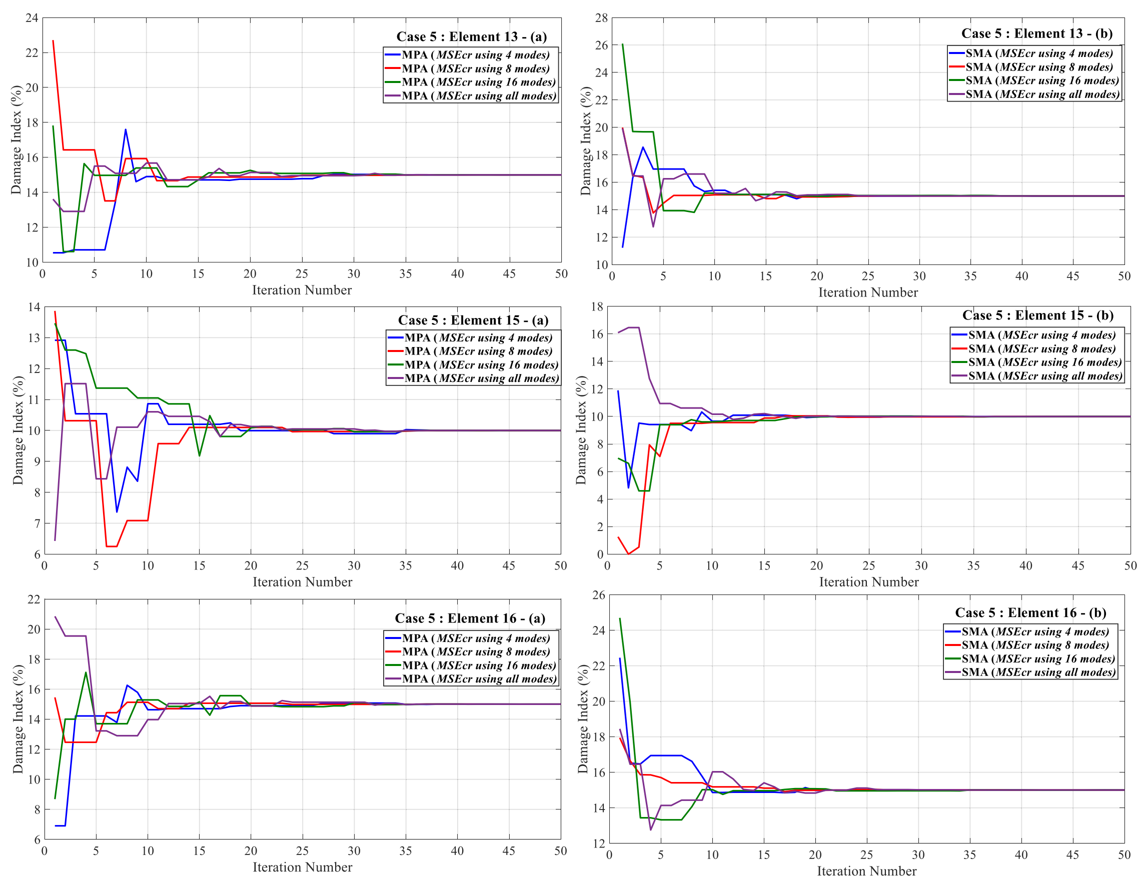

Fig. 19 A convergence study of 31-bar planar Truss—case 5

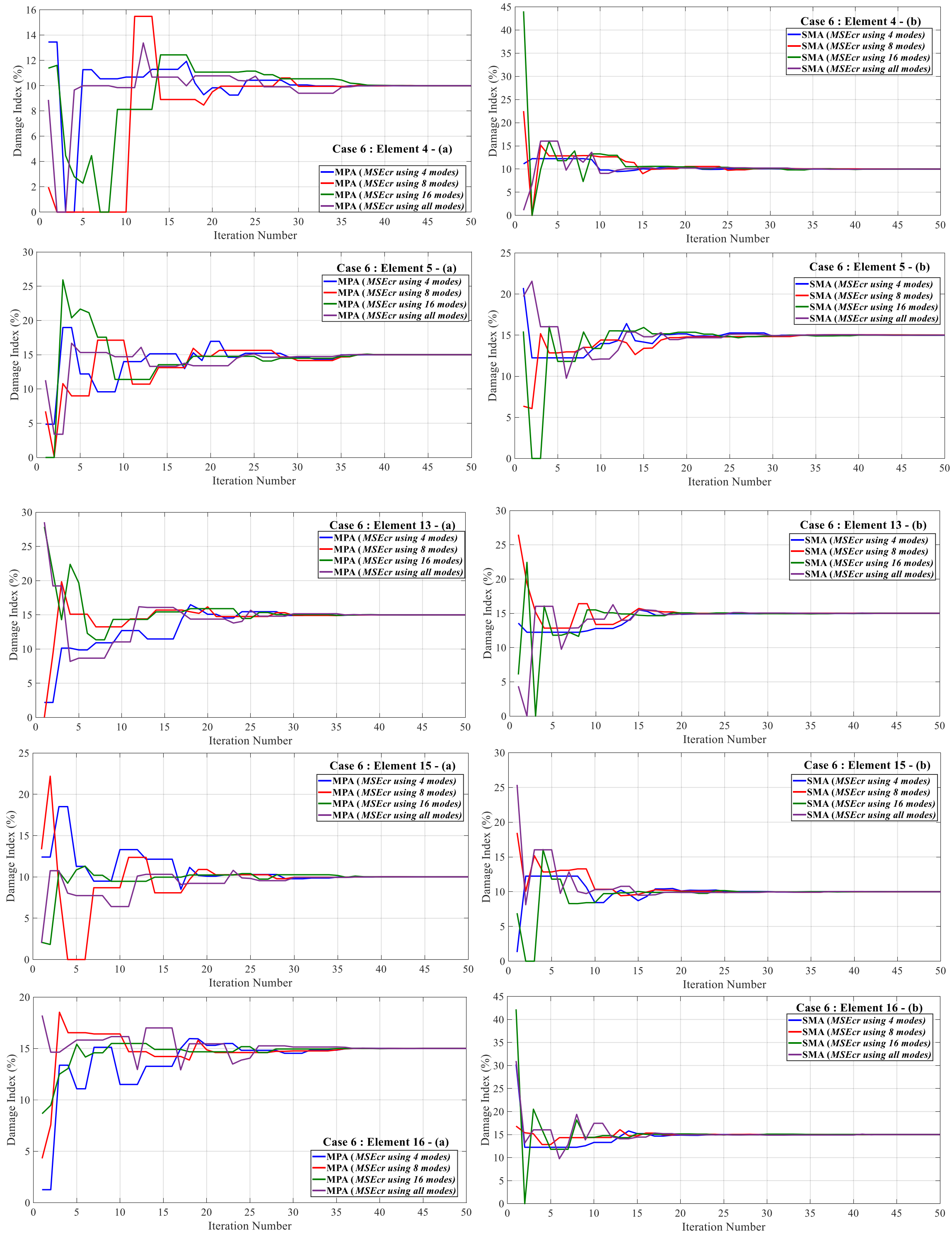

Fig. 20 A convergence study of 31-bar planar Truss—case 6

Table 7 Fitness values for different iterations and different numbers of modes for the 31-bar planar truss using SMA and MPA

Case	Number of modes	Optimization method	Iteration					
			1	10	20	30	40	50
4	4	MPA	1.48	0.579	0.18	0.117	0.0514	0.0167
		SMA	5.22	1.37	0.127	0.117	0.038	0.0142
	8	MPA	3.77	0.519	0.185	0.0396	0.0396	0.000694
		SMA	1.57	1.57	0.447	0.067	0.0147	0.00572
	16	MPA	1.41	0.346	0.0246	0.0246	0.0072	0.0072
		SMA	3.92	0.9	0.375	0.0515	0.0334	0.0106
	All	MPA	2.12	0.36	0.0829	0.0423	0.0207	0.00967
		SMA	1.89	0.642	0.0933	0.0367	0.0367	0.0112
5	4	MPA	16.5	8.77	1.69	0.744	0.52	0.454
		SMA	27.6	4.97	1.3	0.487	0.2	0.0848
	8	MPA	27	9.39	5.69	0.474	0.474	0.11
		SMA	22.2	5.45	0.919	0.66	0.216	0.126
	16	MPA	15.3	3.52	2.16	1.59	0.411	0.277
		SMA	28.6	3.94	0.762	0.54	0.136	0.0921
	All	MPA	5.82	1.98	1.02	0.474	0.176	0.0872
		SMA	8.04	1.48	0.669	0.294	0.1	0.0695
6	4	MPA	29.4	10.4	8.59	7.55	2.74	1.46
		SMA	50.4	8.55	5.73	2.52	0.813	0.439
	8	MPA	45.7	19	11.6	5.41	4.01	1.78
		SMA	47.5	11.2	6.36	3.13	0.719	0.492
	16	MPA	27.2	12.1	4.33	2.51	1.55	1.41
		SMA	66.6	9.67	4.13	1.25	0.638	0.454
	All	MPA	14.1	5.37	4.63	2.38	1.71	0.899
		SMA	22.9	7.05	3.17	0.663	0.334	0.272

Table 8 CPU time (s) for a 31-bar planar Truss

Number of modes	CPU time (s)					
	Case 4		Case 5		Case 6	
	MPA	SMA	MPA	SMA	MPA	SMA
4	119.482111	39.942704	96.161247	43.050094	132.219715	40.192145
8	118.837240	51.901754	120.973400	50.918544	123.969192	49.981278
16	179.229423	70.729241	167.421117	72.039025	178.735362	68.531608
All	207.426206	91.037447	215.329233	89.610000	233.021325	89.399593

obtained from FEM and the measured ones are compared and minimized using the following equation:

$$\mathrm{OF} = \sum_{i=1}^{r} \frac{(\omega_i^c - \omega_i^m)^2}{(\omega_i^m)^2} \quad i = 1, \ldots, r, \tag{16}$$

where r presents the number of modes used in Eq. (16) to formulate the objective function. In this example, four modes are considered to solve the optimization problem. ω_i^m and ω_i^c are the measured (experimental) and calculated (FE model) natural frequencies, respectively. The number of iterations

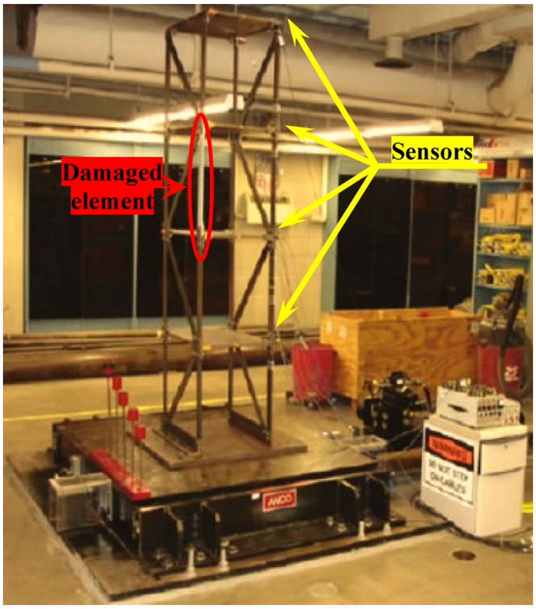

Fig. 21 The four-story shear-type steel frame [35]

Table 9 Natural frequencies (Hz) of the healthy and damaged steel frame

Mode	Initial	Experimental healthy	Updated FEM-SMA	Experimental damaged	FEM damaged
1	3.747	3.902	3.902	3.856	3.856
2	10.788	10.98	10.98	10.808	10.808
3	16.528	18.645	18.645	18.327	18.327
4	20.275	26.243	26.243	25.442	25.442

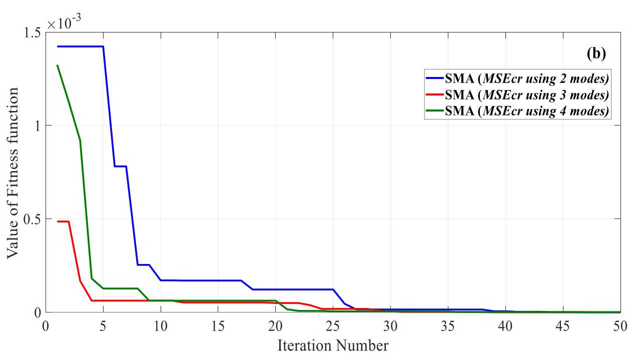

Fig. 22 Evolutionary process using SMA to calibrate FEM based on the experimental steel frame measurements

and population sizes are 50 and 100, respectively. The FE stiffness matrices for the initial model and improved model using SMA are presented in Eqs. 17 and 18, respectively:

$$K_{\mathrm{initial}} = 10^5 \times \begin{bmatrix} 3.4000 & -1.7000 & 0 & 0 \\ -1.7000 & 3.4000 & -1.7000 & 0 \\ 0 & -1.7000 & 3.4000 & -1.7000 \\ 0 & 0 & -1.7000 & 1.7000 \end{bmatrix} (\mathrm{N/m}), \tag{17}$$

$$K_{\mathrm{SMA}} = 10^5 \times \begin{bmatrix} 5.1471 & -3.8735 & 0 & 0 \\ -3.8735 & 6.1124 & -2.2389 & 0 \\ 0 & -2.2389 & 4.0503 & -1.8114 \\ 0 & 0 & -1.8114 & 1.8114 \end{bmatrix} (\mathrm{N/m}). \tag{18}$$

The rigidity matrix, which was optimized using SMA, has been adopted for subsequent calculations of damage detection and quantification. The steel frame's diagonal mass matrix is described as follows:

$$M = \begin{bmatrix} 37 & 0 & 0 & 0 \\ 0 & 37 & 0 & 0 \\ 0 & 0 & 37 & 0 \\ 0 & 0 & 0 & 37 \end{bmatrix} (\mathrm{kg}). \tag{19}$$

The evolutionary FE updating mechanism for the experimental steel frame is shown in Fig. 22. Table 9 summarized the natural frequencies of an initial and improved model using SMA for both healthy and damaged structures.

To get the natural frequencies and mode shapes in the damaged state, modal analysis is also carried out. In Fig. 23, healthy and damaged mode shapes are shown.

From Fig. 24, it can be seen that MSEcr damage indicator can estimate the location of damaged story exactly using different numbers of modes. In addition, SMA algorithm is used as an inverse problem to estimate the severity of damage. The results are plotted in Fig. 25. The number of iteration and population size are 50 and 100, respectively. The fitness values for different iterations and different numbers of modes are summarized in Table 10.

CPU time using different numbers of modes are presented in Table 11. Based on the provided results less number of modes can predict exactly the location of the damaged element using damage indicator. Moreover, less CPU time is required to predict the potential of a damaged element using SMA algorithm.

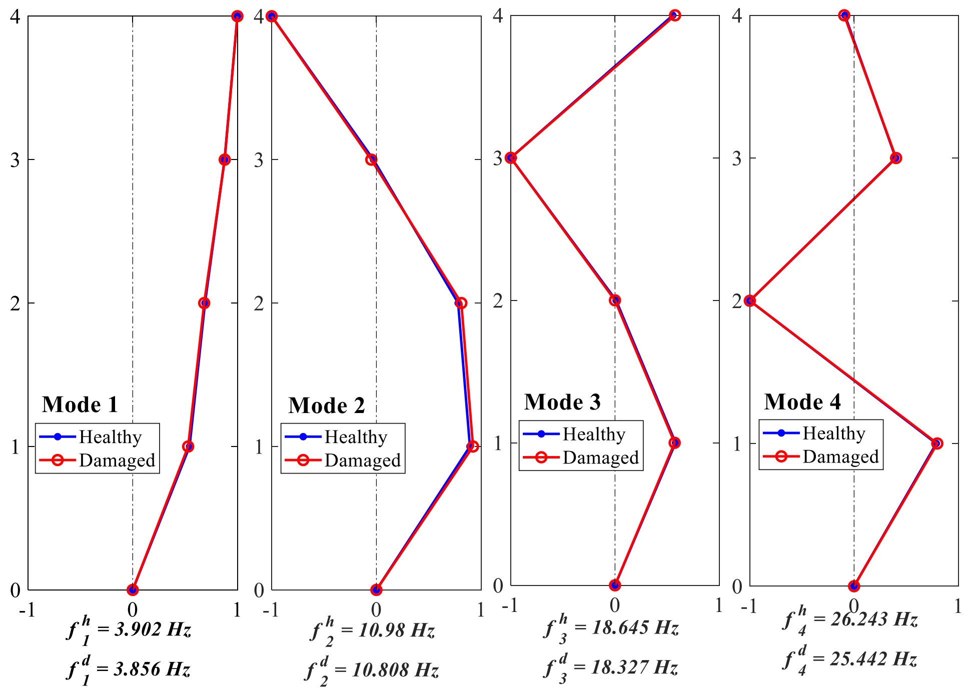

Fig. 23 Mode shapes of the healthy and damaged steel frame

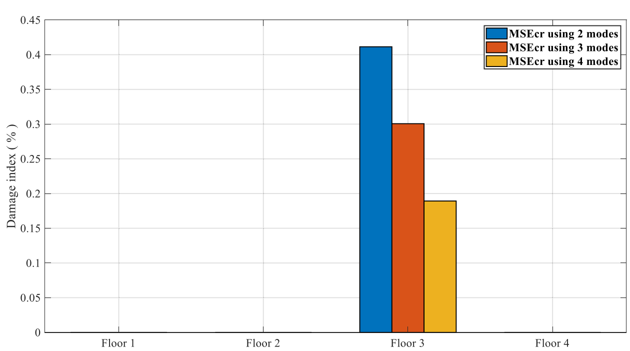

Fig. 24 Damage identification based on an experimental data of the steel frame using MSEcr

6 Noise effect

To study the stability of the proposed approach, we introduced white Gaussian noise with 2% and 4% in case 2 for a simply supported beam (using 8 modes) and case 4 for a 31-bar planar truss (using 8 modes) using SM algorithm.

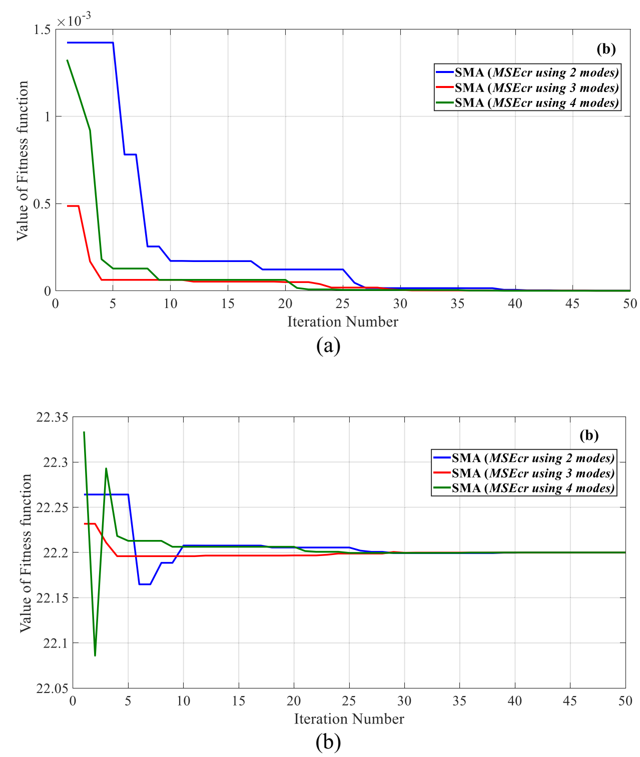

Fig. 25 Damage detection using the experimental data of the four-story shear-type steel frame—**a** convergence of fitness function and **b** Damage Index, respectively

Table 10 Fitness values for different iterations and different numbers of modes

Iteration	Number of modes		
	2	3	4
	SMA	SMA	SMA
1	1.42E−03	4.86E−04	1.32E−03
10	1.71E−04	6.24E−05	6.24E−05
20	1.22E−04	4.96E−05	6.24E−05
30	1.50E−05	4.82E−06	4.55E−06
40	5.55E−06	7.35E−07	1.79E−08
50	2.62E−07	1.98E−08	9.75E−09

Table 11 CPU time for damage detection in the experimental four stories shear-type steel frame

Number of modes	CPU time (s) SMA
2	4.67
3	4.68
4	5.5

$$\varphi_i^{\text{Noise}} = (1 + \sigma\gamma)\varphi_i, \tag{20}$$

where σ is the noise level, γ is a random number in the interval $[-1, 1]$, and φ_i is a ith mode shape.

6.1 A simply supported beam

Noise with 2% and 4% is considered to study the ability of MSEcr and SMA for case 2 using 8 modes. The provided results are presented in Fig. 26, and Figs. 27 and 28 present the fitness and damage index using SMA including noise with 2% and 4%. Tables 12 and 13 summarize the fitness and damage rate for different iterations.

The results showed that SMA can predict the exact location and damage level even for noise 4%.

6.2 A 31-bar planar truss

To test the effectiveness of MSEcr and SMA, noise with 2% and 4% are considered for case 4 using 16 modes. The provided results are presented in Fig. 29, and Figs. 30 and 31 present the fitness and Damage Index using SMA

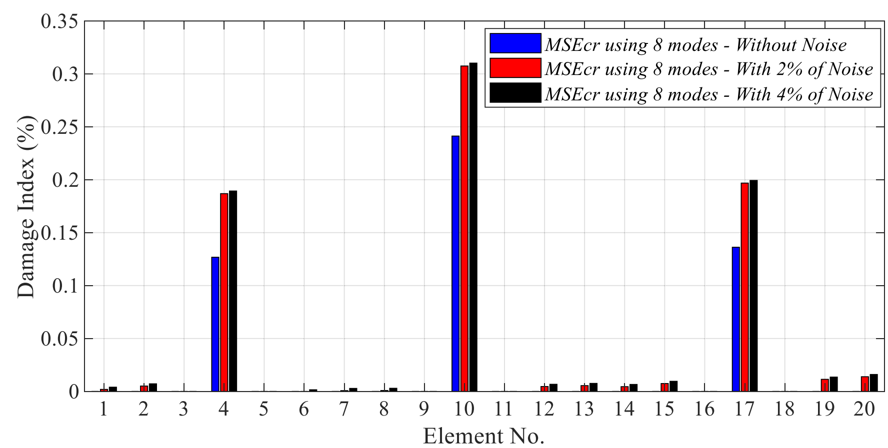

Fig. 26 Damage Index using MSEcr—a simply supported beam—case 2 without and with 2%, 4% noise

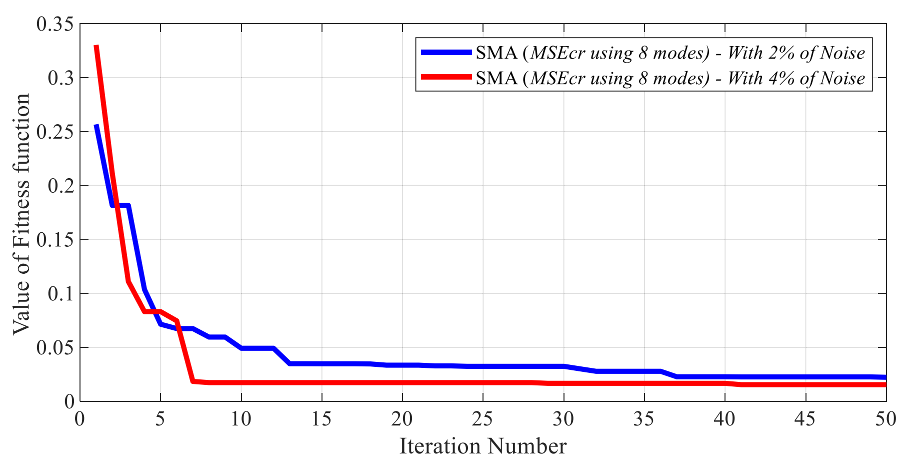

Fig. 27 A simply supported beam: convergence of fitness function of case 2—SMA

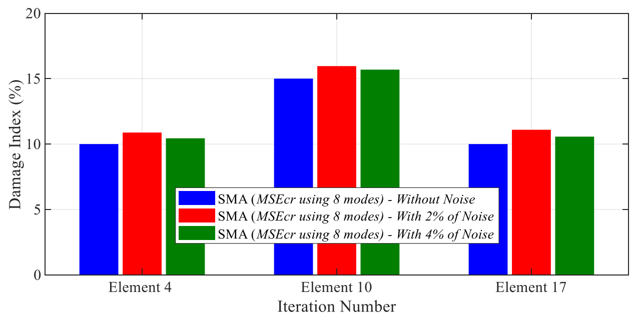

Fig. 28 Damage Index—a simply supported beam—case 2 without and with 2%, 4% noise

Table 12 Fitness values for different iterations—a simply supported beam using 8 modes and SMA

Iteration	Without noise	With 2% noise	With 4% noise
1	11.5621002	0.2567113	0.21517738
10	1.91068512	0.0491728	0.04912169
20	0.2035183	0.03349931	0.02035524
30	0.06412339	0.03242559	0.0195086
40	0.0291202	0.02274178	0.0195086
50	0.00444248	0.02226342	0.0195086

including noise 2% and 4%. Tables 14 and 15 summarize the fitness and damage level for different iterations.

The results for complex 2D structure showed that SMA can predict the exact location and damage level even for noise 4%.

7 Conclusion

This study presents an approach for structural damage detection, localization and quantification focused on modal strain energy change ratio (*MSEcr*) combined with SMA and MPA. Two structures were considered to test the accuracy of the proposed approach, i.e. a simply supported laboratory beam discretized in 20 elements and a bar planar truss modelled with 31 elements. In the first stage, *MSEcr* was used to predict the location of the damaged elements. Furthermore, *MSEcr* was used as an objective function in the second stage using SMA and MPA for damage quantification for the damaged elements predicted in the first stage. Single and multiple damages are investigated based on a different number of modes to study the accuracy of *MSEcr*.

Table 13 Damage Index values for different iterations—a simply supported beam using 8 modes and SMA

	Iteration	1	10	20	30	40	50
Element 4	without Noise	8.62	9.81	10.07	10.00	9.99	10.00
	with 2% Noise	4.85	9.33	10.16	10.78	10.78	10.88
	with 4% Noise	13.16	9.71	10.44	10.44	10.44	10.44
Element 10	without Noise	16.61	15.76	15.00	15.01	15.00	15.00
	with 2% Noise	7.64	16.28	15.06	15.03	15.95	15.96
	with 4% Noise	7.92	16.34	15.69	15.69	15.69	15.69
Element 17	without Noise	4.48	9.77	9.94	10.03	9.99	10.00
	with 2% Noise	16.57	11.58	11.58	11.58	11.01	11.09
	with 4% Noise	14.82	8.47	10.57	10.57	10.57	10.57

Fig. 29 Damage Index—a 31-bar planar truss—case 4 without and with 2%, 4% noise

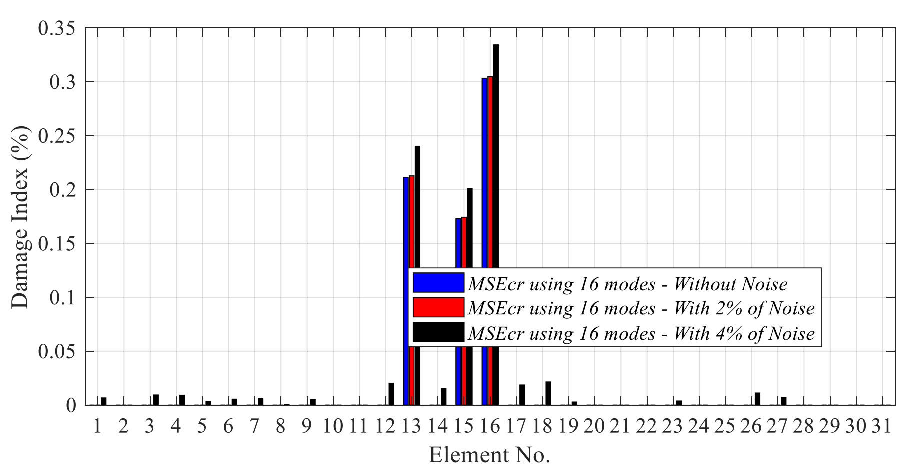

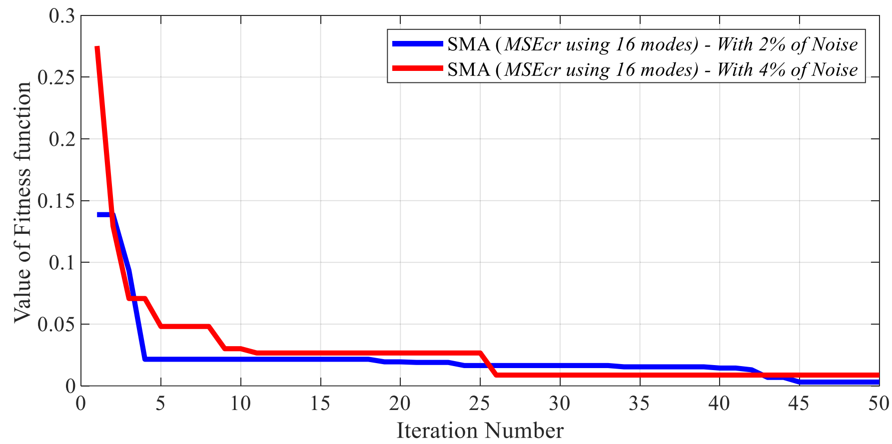

Fig. 30 A 31-bar planar truss: convergence of fitness function of case 4—SMA

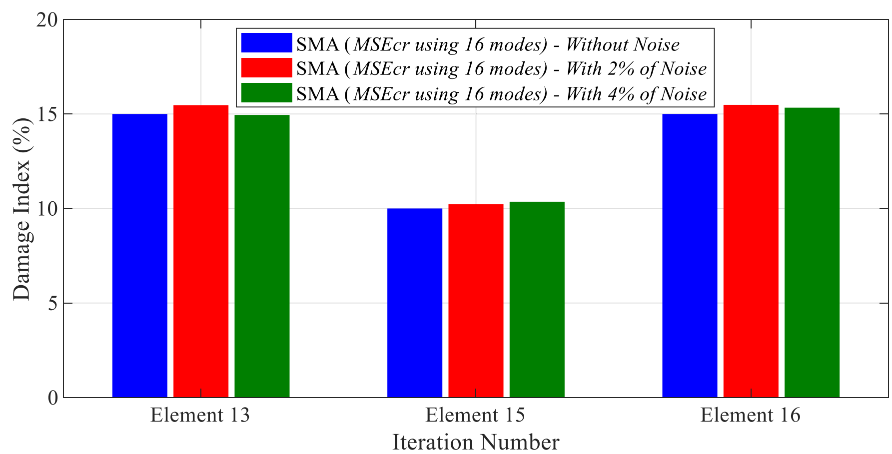

Fig. 31 Damage Index—a 31-bar planar truss—case 4 without and with 2%, 4% noise

Table 14 Fitness values for different iterations—a 31-bar planar Truss using 16 modes and SMA

Iteration	Without noise	With 2% noise	With 4% noise
1	28.6353051	0.13865182	0.27523558
10	0.76159285	0.02153109	0.03007838
20	0.13612041	0.01944276	0.02662174
30	0.08783045	0.01645665	0.00872342
40	0.02416637	0.01441887	0.00872342
50	0.00404462	0.00307027	0.00872342

The experimental results demonstrated that SMA has good convergence performance compared with MPA for different scenarios and structures. Moreover, SMA requires less CPU time compared with MPA. Furthermore, experimental validation was carried out using the data of a four-story steel frame, taken from literature. This confirms the validity and accuracy of the proposed methodology.

Table 15 Damage Index values for different iterations—a 31-bar planar truss using 16 modes and SMA

	Iteration	1 (%)	10 (%)	20 (%)	30 (%)	40 (%)	50 (%)
Element 13	Without noise	26.10	15.21	14.98	15.03	15.01	15.00
	With 2% noise	19.72	13.66	13.60	13.60	16.00	15.47
	With 4% noise	17.55	16.91	14.89	14.95	14.95	14.95
Element 15	Without noise	6.97	9.61	9.97	10.03	9.99	10.00
	With 2% noise	7.47	9.61	9.61	9.70	9.62	10.22
	With 4% noise	17.06	9.56	10.36	10.36	10.36	10.36
Element 16	Without noise	24.70	15.02	15.07	14.96	15.00	15.00
	With 2% noise	12.23	13.74	13.91	14.76	14.85	15.48
	With 4% noise	30.06	15.24	15.24	15.33	15.33	15.33

References

1. Doebling SW, Farrar CR, Prime MB, Shevitz DW (1996) Damage identification and health monitoring of structural and mechanical systems from changes in their vibration characteristics: a literature review. Los Alamos National Lab., NM (United States)
2. Zou Y, Tong L, Steven GP (2000) Vibration-based model-dependent damage (delamination) identification and health monitoring for composite structures—a review. J Sound Vib 230(2):357–378
3. Wang Y-L (2014) New damage localization indicator based on curvature for single-span beams. Struct Eng Mech 51(6):1037–1046
4. Rytter A (1993) Vibrational based inspection of civil engineering structures. Department of Building Technology and Structural Engineering, Aalborg University
5. Yang Q, Liu J (2007) Structural damage identification based on residual force vector. J Sound Vib 305(1–2):298–307
6. Tiachacht S, Bouazzouni A, Khatir S, Wahab MA, Behtani A, Capozucca R (2018) Damage assessment in structures using combination of a modified Cornwell indicator and genetic algorithm. Eng Struct 177:421–430
7. Capozucca R (2009) Static and dynamic response of damaged RC beams strengthened with NSM CFRP rods. Compos Struct 91(3):237–248
8. Cha YJ, Buyukozturk O (2015) Structural damage detection using modal strain energy and hybrid multiobjective optimization. Comput Aided Civ Infrastruct Eng 30(5):347–358
9. Khatir S, Belaidi I, Serra R, Wahab MA, Khatir T (2015) Damage detection and localization in composite beam structures based on vibration analysis. Mechanics 21(6):472–479
10. Khatir S, Belaidi I, Khatir T, Hamrani A, Zhou Y-L, Abdel Wahab M (2017) Multiple damage detection in composite beams using Particle swarm optimization and genetic algorithm. Mechanika 23(4):514–521
11. Nobahari M, Seyedpoor SM (2013) An efficient method for structural damage localization based on the concepts of flexibility matrix and strain energy of a structure. Struct Eng Mech 46(2):231–244
12. Pandey A, Biswas M (1994) Damage detection in structures using changes in flexibility. J Sound Vib 169(1):3–17
13. Tiachacht S, Bouazzouni A, Khatir S, Behtani A, Zhou Y-L-M, Wahab MA (2018) Structural health monitoring of 3D frame structures using finite element modal analysis and genetic algorithm. J Vibroeng 20(1):202–214
14. Samir K, Brahim B, Capozucca R, Wahab MA (2018) Damage detection in CFRP composite beams based on vibration analysis using proper orthogonal decomposition method with radial basis functions and cuckoo search algorithm. Compos Struct 187:344–353
15. Zenzen R, Khatir S, Belaidi I, Le Thanh C, Wahab MA (2020) A modified transmissibility indicator and Artificial Neural Network for damage identification and quantification in laminated composite structures. Compos Struct 248:112497
16. Hwang H, Kim C (2004) Damage detection in structures using a few frequency response measurements. J Sound Vib 270(1–2):1–14
17. Mohan S, Maiti DK, Maity D (2013) Structural damage assessment using FRF employing particle swarm optimization. Appl Math Comput 219(20):10387–10400
18. Yuen MMF (1985) A numerical study of the eigenparameters of a damaged cantilever. J Sound Vib 103(3):301–310
19. Yang Q (2009) A numerical technique for structural damage detection. Appl Math Comput 215(7):2775–2780
20. Ghannadi P, Kourehli SS (2020) Multiverse optimizer for structural damage detection: Numerical study and experimental validation. Struct Des Tall Spec Build 29(13):e1777
21. Ghannadi P, Kourehli SS, Noori M, Altabey WA (2020) Efficiency of grey wolf optimization algorithm for damage detection of skeletal structures via expanded mode shapes. Adv Struct Eng 23(13):2850–2865
22. Khatir S, Wahab MA, Boutchicha D, Khatir T (2019) Structural health monitoring using modal strain energy damage indicator coupled with teaching-learning-based optimization algorithm and isogoemetric analysis. J Sound Vib 448:230–246
23. Khatir S, Dekemele K, Loccufier M, Khatir T, Wahab MA (2018) Crack identification method in beam-like structures using changes in experimentally measured frequencies and particle swarm optimization. Comptes Rendus Mécanique 346(2):110–120
24. Khatir S, Wahab MA (2019) Fast simulations for solving fracture mechanics inverse problems using POD-RBF XIGA and Jaya algorithm. Eng Fract Mech 205:285–300
25. Khatir S, Tiachacht S, Thanh C-L, Bui TQ, Wahab MA (2019) Damage assessment in composite laminates using ANN-PSO-IGA and Cornwell indicator. Compos Struct 230:111509
26. Ghannadi P, Kourehli SS (2021) An effective method for damage assessment based on limited measured locations in skeletal structures. Advances in Structural Engineering 24(1):183–195
27. Ghannadi P, Kourehli SS (2019) Structural damage detection based on MAC flexibility and frequency using moth-flame algorithm. Struct Eng Mech 70(6):649–659
28. Ghannadi P, Kourehli SS (2019) Data-driven method of damage detection using sparse sensors installation by SEREPa. J Civ Struct Health Monit 9(4):459–475
29. Ghannadi P, Kourehli SS (2019) Model updating and damage detection in multi-story shear frames using Salp swarm algorithm. Earthq Struct 17(1):63–73
30. Li S, Chen H, Wang M, Heidari AA, Mirjalili S (2020) Slime mould algorithm: A new method for stochastic optimization. Future Gener Comput Syst 111:300–323
31. Faramarzi A, Heidarinejad M, Mirjalili S, Gandomi AH (2020) Marine Predators Algorithm: A nature-inspired metaheuristic. Expert Syst Appl 152:113377
32. Shahri AH, Ghorbani-Tanha A (2017) Damage detection via closed-form sensitivity matrix of modal kinetic energy change ratio. J Sound Vib 401:268–281
33. Lin J-F, Wang J, Wang L-X, Law S-S (2019) Structural damage diagnosis-oriented impulse response function estimation under seismic excitations. Sensors 19(24):5413
34. Chatzis MN, Chatzi EN, Smyth AW (2015) An experimental validation of time domain system identification methods with fusion of heterogeneous data. Earthq Eng Struct Dyn 44(4):523–547
35. Azam SE, Chatzi E, Papadimitriou C, Smyth A (2017) Experimental validation of the Kalman-type filters for online and real-time state and input estimation. J Vib Control 23(15):2494–2519